J Electroceram (2009) 23:76–79
DOI 10.1007/s10832-008-9538-7

Electrically stable low voltage operating ZnO thin film transistors with low leakage current Ni-doped $Ba_{0.6}Sr_{0.4}TiO_3$ gate insulator

Young-Bae Kim · Jeong-Ung Kim · Duck-Kyun Choi · Jae-Min Hong · Il-Doo Kim

Received: 9 May 2008 / Accepted: 7 July 2008 / Published online: 25 July 2008

Abstract We report on the fabrication of low-voltage ZnO thin-film transistors using 1% Ni-doped $Ba_{0.6}Sr_{0.4}TiO_3$ as the gate insulator. The Ni-doped BST, deposited by RF magnetron sputtering at room temperature, significantly reduced leakage current density to less than 6×10^{-9} A/cm, as compared to a current density of 5×10^{-4} A/cm for undoped BST films at 0.5 MV/cm. The ZnO thin-film transistor with the Ni-doped BST gate insulator exhibited a very low operating voltage of 4 V. The field-effect mobility, the current on/off ratio and subthreshold swing were 2.2 cm^2 V/s, 1.2×10^6, and 0.21 V/dec respectively.

Keywords Transistor · ZnO · Low voltage operation · Gate insulator

Transparent ZnO films are used as active channel materials, which exhibit n-type semiconductor characteristics with high optical transmittance in the visible spectrum and a wide band gap of 3.3 eV [1, 2]. ZnO thin-film transistors (TFTs) are of particular interest because of their potential to replace hydrogenated amorphous or polycrystalline silicon (a-Si/H or poly-Si) TFTs. This potential exists because good quality ZnO polycrystalline films, showing high field-effect mobility can be grown at room temperature. Thus, ZnO-based electronic circuits offer the possibility of low processing costs and good compatibility with plastic substrates [3, 4]. Furthermore, reports have been published on the high performance of ZnO (or doped ZnO) TFTs with moderate field-effect mobility and high on/off ratios in active matrix organic light emitting diode (AMOLED) applications [5, 6].

However, high operating voltages are still a major limitation in portable and battery-powered applications [7]. Therefore, it is important to incorporate a suitable gate insulator to allow for a higher operating current at lower bias voltages. In general, a high permittivity gate dielectric or reduced dielectric thickness is needed to increase the capacitive coupling of the gate electric field to the ZnO channel layer. However, ZnO-TFTs with thin gate dielectrics show poor performance on flexible polymer substrates, which are often characterized by rough surfaces, making these TFTs susceptible to pinhole formation and low manufacturing yields [7]. In order to ensure pinhole-free coverage, the film should be significantly thicker than the roughness of the substrate. Therefore, the use of high-k gate dielectrics with thicknesses over 200 nm is optimal for stable operation of low voltage ZnO-TFTs. While there have been some promising early results for near room temperature grown high-K gate insulators, including barium zirconium titanate (BZT) [8], $Bi_{1.5}Zn_{1.0}Nb_{1.5}O_7$ (BZN) [2, 3, 4], Al_2O_3 [9], HfO_2 [9, 10], and TiO_2 [11], they generally suffer from poor leakage current characteristics at voltages above 5 V. The authors recently developed Mn-doped

Y.-B. Kim
Information Display Research Institute,
17 Haengdang-dong, Seongdong-gu,
Seoul 133-791, Republic of Korea

J.-U. Kim · D.-K. Choi
Division of Material Science and Engineering,
Hanyang University,
17 Haengdang-dong, Seongdong-gu,
Seoul 133-791, Republic of Korea

D.-K. Choi
e-mail: duck@hanyang.ac.kr

J.-M. Hong · I.-D. Kim (✉)
Center for Energy Materials Research,
Korea Institute of Science and Technology,
P.O. Box 131, Cheongryang,
Seoul 130-650, Republic of Korea
e-mail: idkim@kist.re.kr

$Ba_{0.6}Sr_{0.4}TiO_3$ (BST) thin films deposited at room temperature as a potential candidate for gate insulators [12]. The Mn-doped BST films could provide the required high dielectric constant (~24) coupled with enhanced leakage current characteristics. This reduction in leakage current density was achieved through the deep trapping of electrons in the 3% Mn-doped BST films [12]. Acceptor dopants with six-fold coordination [13], such as Mn^{2+} (r_{eff}=0.67 Å) and Mn^{4+} (r_{eff}=0.53 Å), which occupy the B site of the $A^{2+}B^{4+}O^{2-}$ perovskite structure, can be used to suppress the leakage current in BST films. ZnO TFTs using a 3% Mn-doped BST gate insulator showed a field effect mobility of 1.0 cm^2/Vs and low voltage operation of less than 7 V [14]. However, the dielectric behavior of a room temperature deposited Ni-doped BST film used as a gate insulator has not yet been studied. In this work, we introduce Ni-doping to reduce the leakage current of a room-temperature grown BST gate insulator. In this regard, the suitability of a Ni-doped BST film as a gate insulator in the fabrication of low-voltage (~4 V) ZnO-TFTs is investigated.

An undoped target and a 1% Ni-doped BST target with diameters of two inches were prepared by a conventional ceramic powder process. A BST thin film and a 1% Ni-doped BST thin film, both with thicknesses of 200 nm, were deposited on Pt/Ti/SiO_2/Si substrates at room temperature using an RF magnetron sputtering technique. The undoped and the 1% Ni-doped BST films were prepared using fixed power (80 W) in an Ar/O_2 (ratio= 1:1) atmosphere at a total pressure of 50 mTorr. For electrical measurements, 100-nm-thick Pt top electrodes $\left(A = 4 \times 10^{-4}\,cm^2\right)$ were deposited through a shadow mask on top of the BST and the Ni-doped BST films by DC magnetron sputtering. The dielectric properties for the undoped and the Ni-doped BST films were measured at 1 MHz using an HP4192A impedance analyzer. Current–voltage (I–V) characteristics were measured with a semiconductor parameter analyzer (HP4155A). In these measurements, the voltage step and delay time were 0.05 V and 0 s. ZnO-TFTs were fabricated to further demonstrate the advantages of the 1% Ni-doped BST films as gate insulators. First, a 100-nm-thick Cr gate electrode was deposited by DC magnetron sputtering onto a glass substrate. Then, 200-nm-thick 1% Ni-doped BST gate dielectrics were deposited onto the Cr covered glass substrate by RF magnetron sputtering at room temperature. A ZnO channel layer was deposited at room temperature by sputtering at an RF power of 60 W, a working pressure of 20 mTorr, and in a pure Ar gas atmosphere, to a thickness of 100 nm. The transistors were completed by the evaporation of 100 nm-thick Al top contacts through shadow masks to obtain a channel length of 50 μm and width of 2,000 μm. This was followed by annealing at 300°C for 1 hr in a forming gas ambient (5% H_2+95% N_2) to improve the ZnO-TFTs performance. The electrical characterization of the ZnO-TFTs was carried out with an HP4155A precision semiconductor parameter analyzer.

Figure 1 shows the dielectric constant-electric field characteristics of undoped and 1% Ni-doped BST thin films grown on Pt electrodes at room temperature. The undoped and the 1% Ni-doped BST thin films exhibited relatively high dielectric constants of 28.5 and 26.5, respectively. It is likely that the 1% Ni doping on BST films caused a slightly lower dielectric constant due to the lower valence state, i.e. the dominant valence state, of Ni (Ni^{2+}, r_{eff}=0.69 Å) as compared to that of Ti (Ti^{4+}, r_{eff}= 0.605 Å), which occupies an octahedral site of the (Ba,Sr)TiO_3 perovskite structure [15]. The effective dielectric constant ($\varepsilon_r \sim 26.5$) of the 1% Ni-doped BST films remained high enough to achieve low-voltage operation of less than 4 V in ZnO-TFTs. No measurable variation was observed up to voltages of 0.25 MV, ensuring a voltage-independent oxide capacitance.

Figure 2 shows the I–V characteristics of the undoped and the 1% Ni-doped BST thin films measured in a metal–insulator–metal (MIM) configuration as a function of applied bias voltage. The undoped BST thin film showed poor leakage current properties, for example, a low breakdown strength at 0.4 MV/cm. On the other hand, the measured leakage current density of the 1% Ni-doped BST film remained on the order of $\sim 5 \times 10^{-9}$ A/cm^2, even up to an applied electric field of 0.35 MV/cm (7 V), which represents a significant improvement. The breakdown strength was improved by over 2 MV/cm (not shown). It is revealed from spectroscopic ellipsometry and molecular orbital consideration that the lower leakage current in the 1% Ni-doped BST films is attributed to shallower defect level and lower defect density below the conduction band

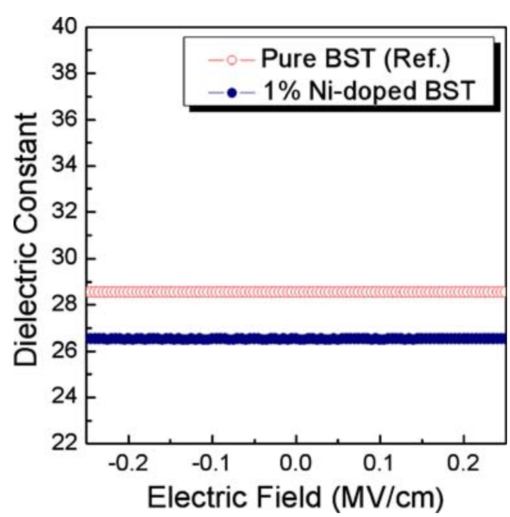

Fig. 1 Dielectric constant-electric field characteristics of pure BST and 1% Ni-doped BST films with the MIM (metal–insulator–metal) configuration

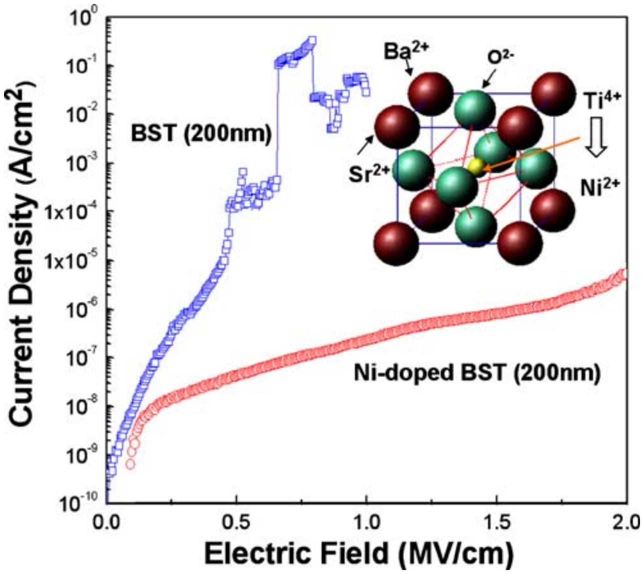

Fig. 2 Current density-electric field characteristics of pure BST and 1% Ni-doped BST films. The inset emphasizes a schematic structure for Ni substitution into the Ti site in the $Ba_{0.6}Sr_{0.5}TiO_3$ lattice

edge than undoped BST thin film (Seo et al., unpublished data).

Figure 3 shows AFM (atomic force microscopy) images of the surface morphology of the undoped and the 1% Ni-doped BST films. The RMS values (standard deviation from the average height of the surface) on 5×5 μm of the undoped and 1% Ni-doped BST films were 1.094 and 0.68 nm, respectively. The 1% Ni-doped BST film exhibited a smoother surface, which can induce good interface characteristics and stable ZnO-TFT operation.

To investigate the advantages of the 1% Ni-doped BST films as gate insulators, ZnO-TFTs were fabricated on glass substrates. A schematic cross-sectional view of our device is shown in Fig. 4(a).

Figure 4(b) shows the drain-to-source current (I_{DS}) as a function of drain-to-source voltage (V_{DS}) at various gate voltages in ZnO-TFTs with 1% Ni-doped BST gate insulators. The ZnO-TFTs exhibited normal off-behavior, which operates via the accumulation of carriers. We conclude that the carriers are electrons because I_{DS} is nonzero for positive V_{DS}. The relatively high capacitance of the 1% Ni-doped BST gate insulators resulted in a low-voltage operation of 4 V. Good current saturation and a high on-current of 53 μA at the bias condition (V_{GS}=4 V and V_{DS}= 5 V) were observed. Figure 4(c) shows the transfer characteristics of the ZnO-TFTs. The threshold voltage (V_{th}) was calculated from the x-axis intercept of the square root of the I_{DS} vs. V_{GS} plot. The field-effect mobility (μ_{FE}) modeled by the equation, $I_{DS} = (WC_i/2L)\mu_{FE}(V_{GS} - V_{th})^2$,

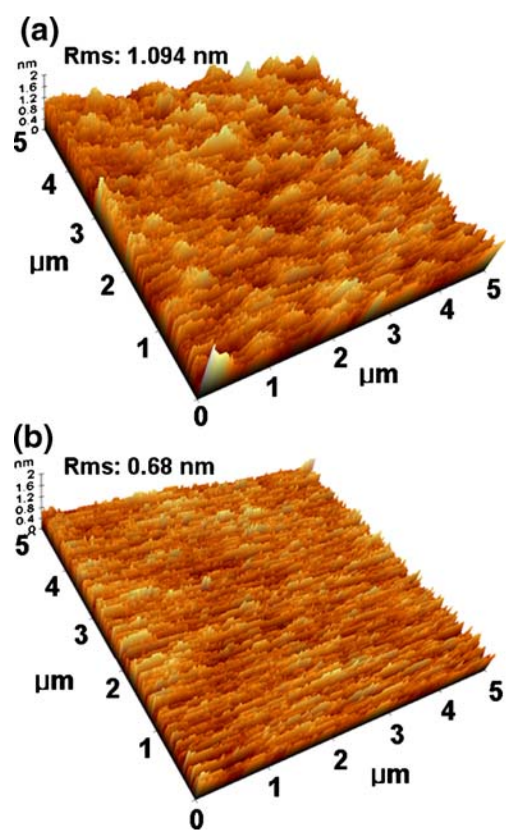

Fig. 3 AFM images of the surface morphology of (**a**) pure BST, and (**b**) 1% Ni-doped BST films

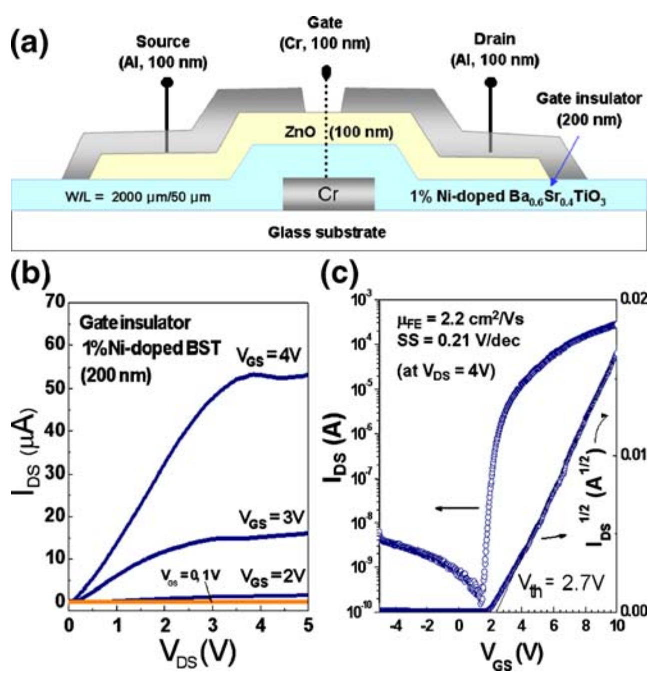

Fig. 4 (**a**) Schematic cross-sectional view of ZnO-TFTs structure with 200 nm-thick 1% Ni-doped BST gate insulator, (**b**) Drain-to-source current (I_{DS}) vs drain-to-source voltage (V_{DS}) curves at various gate-to-source voltages (V_{GS}) for ZnO-TFTs with 1% Ni-doped BST gate insulators on glass substrates [channel length (L) of 50 μm and channel width (W) of 2,000 μm]. (**c**) Transfer characteristics. V_{GS} was swept from −5 to 10 V at a V_{DS} of 4 V

can be calculated from the slope of the plot of $|I_{DS}|^{1/2}$ versus V_{GS} in the saturation region (V_{GS}=4 V), where L is the channel length, W is the channel width, C_i is the capacitance per unit area of the insulating layer, V_{th} is the threshold voltage, and μ_{FE} is the field-effect mobility. The measured V_{th} and μ_{FE} were +2.7 V and 2.2 cm^2/Vs for ZnO-TFTs with a 1% Ni-doped BST gate insulator. The measured subthreshold swing was 0.21 V/dec. The on-current and off-current ratios were 1.86×10^{-4} and 2.90×10^{-9} A, giving an on/off current ratio of 1.2×10^{6}.

In summary, 1% Ni-doped BST films with a high dielectric constant ($\varepsilon_r \sim 26.5$) and low leakage current ($<\sim5\times10^{-9}$ at 7 V) were prepared at room temperature by RF sputtering. A reduction in leakage current density was achieved through shallower trap level and lighter trap density in 1% Ni-doped BST films. ZnO-TFTs using the 1% Ni-doped BST gate insulators (200 nm) exhibited low-voltage operation of less than 4 V and a high field-effect mobility of 2.2 cm^2/Vs. The results of this work demonstrate the potential for use of a 1% Ni-doped BST film as a high-k gate insulator for low-voltage ZnO thin-film transistors.

Acknowledgement We gratefully acknowledge support from KIST Program under Grant No. 2E20792 and Seoul R&BD program under Grant No. 2G07270. This research was supported by the grant (F0004111) from the Information Display R&D Center, one of the 21st Century Frontier R&D Program funded by the Ministry of Knowledge Economy of the Korean Government.

References

1. E.M.C. Fortunato, P.M.C. Barquinha, A.C.M.B.G. Pimentel, A.M.F. Goncalves, A.J.S. Marques, L.M.N. Pereira et al., Adv. Mater. **17**, 590 (2005). doi:10.1002/adma.200400368
2. I.D. Kim, Y.W. Choi, H.L. Tuller, Appl. Phys. Lett. **87**, 042509 (2005). doi:10.1063/1.1995944
3. I.D. Kim, M.H. Lim, K.T. Kang, H.G. Kim, S.Y. Choi, Appl. Phys. Lett. **89**, 022905 (2006). doi:10.1063/1.2220485
4. M.H. Lim, K.T. Kang, H.G. Kim, I.D. Kim, Y.W. Choi, H.L. Tuller, Appl. Phys. Lett. **89**, 202908 (2006). doi:10.1063/1.2387985
5. H. Yabuta, M. Sano, K. Abe, T. Aiba, T. Den, H. Kumomi et al., Appl. Phys. Lett. **89**, 112123 (2006). doi:10.1063/1.2353811
6. P.F. Carcia, R.S. McLean, M.H. Reilly, G. Nunes, Appl. Phys. Lett. **82**, 1117 (2003). doi:10.1063/1.1553997
7. Y.W. Choi, I.D. Kim, H.L. Tuller, A.I. Akinwande, IEEE Trans. Electron. Dev. **52**, 2819 (2005). doi:10.1109/TED.2005.859594
8. C.D. Dimitrakopoulos, S. Purushothaman, J. Kymissis, A. Callegari, J.M. Shaw, Science **283**, 822 (1999). doi:10.1126/science.283.5403.822
9. Y. Kwon, Y. Li, Y.W. Heo, M. Jones, P.H. Holloway, D.P. Norton et al., Appl. Phys. Lett. **84**, 2685 (2004). doi:10.1063/1.1695437
10. P.F. Carcia, R.S. McLean, M.H. Reilly, Appl. Phys. Lett. **88**, 123509 (2006). doi:10.1063/1.2188379
11. L.A. Majewski, R. Schroeder, M. Grell, Adv. Mater. **17**, 192 (2005). doi:10.1002/adma.200400809
12. K.T. Kang, M.H. Lim, H.G. Kim, Y. Choi, H.L. Tuller, I.D. Kim et al., Appl. Phys. Lett. **87**, 242908 (2005). doi:10.1063/1.2139838
13. R.D. Shannon, Acta Crystallogr. A **32**, 751 (1976). doi:10.1107/S0567739476001551
14. K.T. Kang, I.D. Kim, M.H. Lim, H.G. Kim, J.M. Hong, Thin Solid Films **516**, 1218 (2008). doi:10.1016/j.tsf.2007.05.068
15. R.D. Levi, Y. Tsur, Adv. Mater. **17**, 1606 (2005). doi:10.1002/adma.200401859